Brain, Behavior, and Immunity 99 (2022) 157–165

Contents lists available at ScienceDirect

Brain Behavior and Immunity

journal homepage: www.elsevier.com/locate/ybrbi

Dynamics of temperature change during experimental respiratory virus challenge: Relationships with symptoms, stress hormones, and inflammation

Jeffrey Gassen *, Tomasz J. Nowak, Alexandria D. Henderson, Michael P. Muehlenbein

Department of Anthropology, Baylor University, Waco, TX, United States

ARTICLE INFO

Keywords:
Fever
Dynamic structural equation modelling
Time series analysis
Inflammation
Stress
Catecholamines
Cortisol
Cytokines
Body temperature

ABSTRACT

Thermoregulation is a complex, dynamic process involving coordination between multiple autonomic, endocrine, and behavioral mechanisms. In the context of infection, this intricate machinery generates fever, a process believed to serve vital functions in the body's defense against pathogens. In addition to increasing core temperature, infection can lead to changes in the dynamic fluctuations in body temperature over time. The patterns of these deviations may convey information about the health of the body and the course of illness. Here, we utilized dynamic structural equation modeling to explore patterns of body temperature change following an experimental respiratory virus challenge in an aggregated, archival dataset of human participants ($N = 1{,}412$). We also examined whether temperature dynamics during infection were related to symptom severity, as well as individual differences in biomarkers of inflammation and stress. We found that individuals meeting the criteria for infection exhibited higher but less stable body temperatures over time compared to those not meeting criteria of infection. While temperature parameters did not reliably predict symptom severity, higher levels of nasal proinflammatory cytokines were associated with lower, more consistent temperatures during the study period. Further, levels of salivary cortisol and urinary catecholamines measured at the beginning of the study appeared to have disparate effects on temperature change. In sum, this research highlights the utility of dynamic time series modeling as a framework for studying body temperature change and lends novel insights into how stress may interact with infection to influence patterns of thermoregulation.

1. Introduction

In homeotherms, thermoregulation is a complex, dynamic process that involves coordination between multiple physiological systems to maintain core temperature within a homeostatic window (Angilletta et al., 2010; Jessen, 2012). Thermoreceptors in the skin, viscera, and central nervous system are responsible for monitoring internal and ambient temperatures. This information is relayed to the brain, namely the preoptic area (POA) of the hypothalamus, which triggers a series of physiological and behavioral shifts to combat current (i.e., deviations from normal internal temperature) or expected (i.e., ambient conditions above or below normal internal temperature) thermal challenges (Gagge, 2011; Ravanelli et al., 2019; Rezende and Bacigalupe, 2015). For example, defenses against excessive heat include autonomic responses to facilitate heat loss, such as elevated cardiac output, vasodilation, and sweating, as well as motivation to seek out cooler environments. On the contrary, responses to excessive cold include brown adipose tissue thermogenesis (although not for all homeotherms), vasoconstriction, and behavioral outputs like shivering or seeking out heat, each of which function to increase core temperature or minimize heat loss (Angilletta et al., 2010; Jessen, 2012; Gagge, 2011; Ravanelli et al., 2019; Rezende and Bacigalupe, 2015).

While humans' normothermic range is approximately 96.31–99.97°F (35.73–37.76 °C; (Geneva et al., 20192019), higher or lower levels are often temporarily maintained in response to certain internal and environmental stressors (Ramsay and Woods, 2014; Verburg-van Kemenade et al., 2017). Perhaps the most well-described example of these allostatic temperature shifts is the febrile response (Biddle, 2006; GENSINI and CONTI, 2004). When infection is detected, macrophages and other sentinel cells release pyrogenic cytokines, such as interleukin-1 beta (IL-1β), IL-6, and tumor necrosis factor alpha (TNF-α), that induce the production of prostaglandins (namely PGE2) in the hypothalamus. In

* Corresponding author at: Department of Anthropology, Baylor University, One Bear Place #97173, Waco, TX 76798, United States.
E-mail address: jeffrey_gassen@baylor.edu (J. Gassen).

https://doi.org/10.1016/j.bbi.2021.10.001
Received 21 June 2021; Received in revised form 7 September 2021; Accepted 1 October 2021
Available online 6 October 2021

turn, PGE2 acts on neurons in the POA to raise the body's temperature set point, triggering the aforementioned constellation of autonomic, endocrine, and behavioral mechanisms that together promote heat generation and minimize heat loss (BLATTEIS and SEHIC, 1998; Coiffard et al., 2021; Saper and Breder, 1992;93:419–28). Several studies have found that fever serves important adaptive functions by enhancing the effectiveness of immune responses (Evans et al., 2015), mitigating damage to host tissues (Schieber et al., 2016), and limiting the infectivity of certain pathogens (Small et al., 1986).

In the context of infection, the architecture of natural, temporal fluctuations in temperature also tends to change (Harding et al., 2019; Heller et al., 2011; Refinetti and Menaker, 1992; Geneva and Javaid, 2020; Huitron-Resendiz et al., 2007; Zhuang et al., 2017). For example, the circadian phase position (time of temperature peak) is often shifted in patients admitted to the intensive care unit with an infection (Coiffard et al., 2021). Moreover, recent research suggests that the shape and magnitude of these temporal deviations convey information about the type of infection (Cuesta-Frau et al.,) and may even provide prognostic information about morbidity and mortality (Drewry et al., 2013). In other words, analyzing temporal patterns of temperature change, in addition to merely monitoring absolute values, holds promise to enrich understanding of the body's response to infectious pathogens. For instance, one study found that abnormally large swings in daily body temperature were predictive of sepsis diagnosis in afebrile patients admitted to an intensive care unit (Drewry et al., 2013).

Despite these recent advancements, little is known about whether factors like psychological stress impact the temporal dynamics of fever, and if so, the biological mechanisms through which this occurs. For example, the autonomic nervous system plays key roles in both thermoregulation (Angilletta et al., 2010; Jessen, 2012) and the body's response to stress (Ziegler et al., 2012). Additionally, catecholamine receptors are found on several leukocyte subsets where they regulate the release of cytokines, including pyrogens involved in coordinating the febrile response (Mills et al., 1998; Szelenyi and Vizi, 2007). Accordingly, it is possible that stress-induced shifts in autonomic activity influence body temperature changes during infection. Glucocorticoids (such as cortisol) might also mediate relationships between stress and the febrile response given their potent immunomodulatory properties (Riccardi et al., 2002) and importance for energy mobilization (Kuo et al., 2016). The latter possibility is particularly compelling given the steep energetic costs of even small increases in core temperature (Barr et al., 1922; Elia, 1992; Muehlenbein et al., 2010).

In the current project, we sought to characterize within-person dynamics of body temperature change following an experimental respiratory virus challenge and examine how these shifts relate to symptom severity, levels of inflammation (i.e., nasal cytokines), and other features of illness. We also explored whether pre-challenge levels of stress hormones (urinary catecholamines and salivary cortisol) influenced temperature change throughout infection. To estimate a comprehensive set of parameters that model the degree and pattern of variation in body temperature over time, we utilized the recently developed framework of dynamic structural equation modeling (DSEM) (Asparouhov et al., 2018). Such an approach is particularly powerful when analyzing intensive longitudinal data with a large number of within-individual measurements (e.g., time series modeling) for which the majority of individuals' time-varying scores do not conform to a common linear, or even non-linear (e.g., quadratic), trajectory of change. In addition to modeling individuals' average and peak temperatures, this technique allowed us to examine aspects of time-dependent variation, such as autoregressive relationships and residual variance thereof, that are not represented in the estimation of random intercepts and slopes as is commonly employed when analyzing longitudinal biological data (Harrison et al., 2018).

2. Methods

2.1. Procedure

All data were collected as part of the Common Cold Project (CCP) by the Laboratory for the Study of Stress, Immunity, and Disease (2016) at Carnegie Mellon University under the directorship of Sheldon Cohen, Ph.D. Deidentified data are publicly available via the CCP website (www.commoncoldproject.com; grant number NCCIH AT006694). The measures used for this study were part of the aggregated dataset, which included combined data from all five studies of the CCP: (1) the British Cold Study (conducted between 1986 and 1989, $n = 399$), (2) the Pittsburgh Cold Study 1 (PCS 1; conducted between 1993 and 1996, $n = 276$), (3) the Pittsburgh Cold Study 2 (PCS 2; conducted between 1997 and 2001, $n = 334$), (4) the Pittsburgh Mind-Body Center Study (PMBC; conducted between 2000 and 2004, $n = 193$), and (5) the Pittsburgh Cold Study 3 (PCS 3; conducted between 2007 and 2011, $n = 213$). However, some of the variables included in the analyses were not measured in every participant (e.g., subjective symptoms of cold, serology). Accordingly, we list the sample size for each measure used in the current analyses in Table S1.

All studies included in the CCP were prospective viral-challenge studies that involved exposing participants via nasal drops to one of nine viruses responsible for the common cold. These viruses included: (1) rhinovirus (RV) type 2 ($n = 86$), (2) RV9 ($n = 126$), (3) RV14 ($n = 92$), (4) RV23 ($n = 106$), (5) RV39 ($n = 743$), (6) coronavirus 229E (CV229E; $n = 55$), (7) respiratory syncytial virus (RSV, $n = 40$), (8) RV strain Hanks ($n = 129$), and (9) influenza A ($n = 38$). Following exposure, participants were kept in quarantine for 5–6 days (depending on the study), during which the development and course of upper respiratory infections were monitored. In addition, a wide range of demographic, health, psychobehavioral, and biological measures were collected prior to, during, and after quarantine. For reference, the timeline for collection of key variables included in the current research is displayed in Table S1.

2.2. Participants

The aggregated CCP data include a combined sample size of 1,415 participants (655 men, 760 women; $M_{age} = 31.57$ years, $SD = 10.48$). Additional characteristics of the samples for each study have been published elsewhere (Cohen et al., 2006; Cohen et al., 2012; Doyle et al., 2010) (see www.commoncoldproject.com for the full list of publications). Volunteers in each study underwent extensive screening, and only those meeting the following criteria were eligible to participate: 1) proficient in the English language, 2) in good general health as determined by physical examination and medical history, 3) non-pregnant or lactating (females), 4) not taking regular medications, and 5) free of recent illness. Volunteers received monetary compensation in exchange for completing full study protocols. Informed consent was collected prior to participation; all studies received institutional review board approval.

2.3. Materials

2.3.1. Assessment of infection

All five studies determined infection status based on previously described criteria (Gwaltney et al., 1989). Specifically, infection was confirmed if either the challenge virus was recovered in a participant's nasal secretions on any post-challenge quarantine day, or a four-fold increase in serum challenge virus-specific titers was observed 28 days later.

2.3.2. Body temperature

In all five studies, body temperature was measured pre-challenge throughout the first day of quarantine (Q), as well as throughout each

subsequent day of quarantine, using an oral digital thermometer (BCS, PCS 1; IVAC, San Diego, CA) or electronic ear thermometer (PCS 2, PCS 3, PMBC; Braun Thermoscan 6021, WelchAllyn). Temperatures were recorded in the morning (6:00–8:00 AM) and afternoon (12:00–4:00 PM) each day. In PCS 2, PCS 3, and PMBC, a third measurement was taken in the evening (7:00–9:00 PM). Further, while data for days Q0–Q5 were available for all studies, data for Q6–Q8 were only included in a subset of the studies. To minimize the amount of missing data that may compromise reliable estimation of the primary model's key parameters, we only analyzed morning and afternoon data for Q0–Q5, as these data were included in every study. All temperature data were converted to Fahrenheit prior to data analysis.

2.3.3. Pre- and post-challenge antibody levels

The methods for determining challenge virus-specific antibodies differed between the BCS and remaining studies. For the BCS, serum was separated from participants' whole blood collected 1–2 days prior to the viral challenge, as well as 28 days after the challenge, and assayed for levels of virus-specific immunoglobulin A (IgA) and immunoglobulin G (IgG) using enzyme-linked immunosorbent assays (ELISAs). The protocols for determining circulating antibody levels to the challenge virus also differed between the RVs included in this particular study (Barclay and Al-Nakib, 1987; Al-Nakib et al., 1988). However, in both cases, sample assay values were corrected for dilution and control values, and then categorized as quantitative titers based on optical density values: < 1:2, 1:2 or < 1:4, 1:4 or < 1:8, 1:8 or < 1:16, 1:16 or > 1:16, 1:32, and 1:64. A full description of the methods can be found on the Common Cold Project website.

For the remaining studies, serum antibody levels to the challenge virus were determined using microtiter neutralization assays for rhinovirus (Al-Nakib et al., 1988) and a hemagglutination inhibition assay (Lennette and Schmidt, 1979) for influenza A. For PCS 1, pre-challenge antibody levels were assayed from samples collected one week prior to quarantine, while samples were collected 60 days or 3–5 days before quarantine for PCS 2 and PCS 3, respectively. For the PMBC, pre-challenge samples were collected on the first day of quarantine, prior to inoculation with the virus. For the BCS, post-challenge whole blood samples were collected 28 days after inoculation, and data were reduced to the same quantitative titer range based on serial dilution. Given the numerous differences in protocols between studies and challenge viruses, we controlled for both study and type of virus in the present analyses.

2.3.4. Mucus weight

For PCS 1, PCS 2, PMBC, and PCS 3, mucus weight was measured as a quantitative, objective symptom of cold. Each day of quarantine, participants expelled nasal secretions into pre-weighed tissue paper and sealed them in plastic bags. In the evening, research staff collected the bags containing these tissues and weighed them again. Adjusted daily mucus production was calculated by subtracting the baseline weight of the tissues from the total weight at the end of the day. For the current study, total mucus weight (g) was computed as the sum of adjusted mucus weights from all days of quarantine.

2.3.5. Viral shedding

For all CCP studies, daily nasal wash samples were assayed for the presence of the challenge virus (and non-challenge rhinovirus strains on Q0-Q1 for PCS 1–3). The presence of RVs and CV229E were confirmed by neuralization tests (Al-Nakib et al., 1989), RSV was confirmed through immunofluorescent staining of target cells (McQuillin and Gardner, 1968), and influenza A was confirmed by a hemagglutination inhibition assay (Tobita et al., 1975). The variable used in the present study was the total number of days that the challenge virus was detected in a participant's nasal wash.

2.3.6. Self-reported symptoms of cold

To measure subjective symptoms of cold in the four most recent studies, participants rated the severity of eight physical manifestations of cold-related illness (0 = lowest severity, 32 = highest severity), including nasal congestion, sneezing, runny nose, sore throat, cough, headache, chills, and malaise (Jackson et al., 1958). The pre-challenge severity rating was subtracted from each daily rating to compute an adjusted symptom score; scores across quarantine days were summed to create a total symptom severity variable.

2.3.7. Nasal cytokine response

In PCS 1, PCS 2, PMBC, and PCS 3, the nasal wash samples described above were assayed in duplicate for levels of several cytokines using ELISAs (PCS 1, PCS 2, PCS 3) or multiplex technology (PMBC). See the Common Cold Project website for manufacturer information. In the aggregated dataset used for the current research, data were available for levels of IL-1β, IL-6, IL-8, TNF-α, and interferon-alpha (IFN-α).

In PCS 1, nasal wash samples were assayed only for IL-8. All assays were conducted at the Immunologic Monitoring and Cellular Products Laboratory (IMCPL) at the University of Pittsburgh Cancer Institute. The institute has internal standards for assay sensitivity and reliability. Accordingly, inter-and intra-assay coefficients of variation were not reported with the public data. The CCP researchers computed the area under the curve (AUC) values for levels of each cytokine across the study period. Given the nature of the computation, these values are only available for participants without missing data. Some of the correlations between cytokine AUCs were very high (Pearson's $r > 0.95$). Accordingly, we modeled these cytokines together as a latent factor to avoid multicollinearity in the regression analysis. Latent factors are used to mathematically model unobserved constructs represented, or "indicated", indirectly by multiple observed variables that are related (Muthén, 2002). In this case, levels of the five different cytokines together represent the overall construct of inflammation, which itself cannot be observed directly. The extent to which each observed variable is related to the overall latent factor is typically determined by a standardized factor loading representing coefficients from the regression of the observed variable on the construct overall. Any composite measure of a scale or set of variables can be thought of as a latent factor. For example, computing a mean composite of related items from a validated scale yields a latent variable with perfect and equal factor loadings across observed variables and residual variances of 0. In other words, variance in each item is assumed to be completely explained by the composite measure. Conversely, the advantage of the latent variable modeling framework employed here is that variability in factor loadings and error are included as part of the model.

2.3.8. Salivary cortisol levels

Salivary cortisol data were available for PCS 2, PMBC, and PCS 3. A detailed description of saliva collection protocols is available on the Common Cold Project website. For PCS 2, 11 saliva samples were collected on each of the two days preceding viral challenge, starting immediately upon waking and ending 16 h later. Participants in this study provided an additional 14 samples on Q0. The collection protocol for PMBC and PCS 3 resembled PCS 2; however, only seven saliva samples were collected on each of the two days prior to quarantine (starting one hour after awakening and ending 11 h later), and eight samples were collected on Q0. The aggregated CCP dataset only includes PCS 2 data from time points that match the subsequent studies in order to establish equivalence.

Saliva samples for PMBC were assayed in duplicate for cortisol levels using commercially available ELISAs. CCP researchers reported that correlations between original and repeat samples exceeded $r = 0.96$, and average intra-assay CVs were 4%. Saliva samples for PCS 2 and PCS 3 were assayed in duplicate using time-resolved fluorescence with a cortisol-biotin conjugate as a tracer (Dressendörfer et al., 1992). Intra- and inter-assay CVs were<12%. Similar to the nasal wash cytokine level

data, AUC values were calculated for each day of saliva collection for participants without missing data. For the present study, we used cortisol AUC values for saliva collected on Q0, the same day temperature was first monitored.

2.3.9. Urinary catecholamine levels

For PCS 1, PCS 2, and PMBC, 24-hour urine samples were collected during the first day of quarantine. An additional 24-hour sample was collected prior to quarantine for participants in PCS 2 and PMBC. Urine samples were later assayed for levels of norepinephrine, epinephrine, and dopamine using high-performance liquid chromatography with reported inter-assay CVs below 4%. Creatinine was measured to correct for daily urine excretion. The variables analyzed in the present study were 24-hour urinary levels of each catecholamine (mcg) divided by creatinine levels (mg). For participants with two samples, the variables analyzed were the average of the two values. Levels of the three catecholamines were highly correlated (Pearson's *rs*: 0.77-0.92). Accordingly, we modeled these together as a latent factor representing urinary catecholamine output.

2.3.10. Covariates

A number of demographic, health, behavioral, and environmental variables were included in the present analyses that may be associated with the dynamics of individuals' body temperature changes in the context of a viral challenge. These included body mass index (BMI), age, sex, race/ethnicity, subjective socioeconomic status (SES) in the local community, parents' level of education (i.e., as an estimate of childhood SES; mean of both parents), smoking status, physically active (times per week), sleep duration and efficiency (Pittsburgh Sleep Quality Index; (Buysse et al., 1989), and season of trial.

2.4. Data analysis plan

All models were estimated using MPlus statistical software (Muthén, 2010). Missing data (see Table S1 for variable-specific *n*) were handled using maximum likelihood estimation. All available data were included in the analyses. As is common for biological data, the mucus weight, subjective symptoms, cytokine, cortisol, and catecholamine data were all positively skewed. However, credibility intervals—interpreted in a similar fashion as confidence intervals—were generated by Bayesian estimation for each effect; these intervals do not require normal parameter distributions (see below for more information) (Muthén, 2010). Accordingly, variables were not transformed as leaving them with their observed distributions was unlikely to bias parameter estimation and yielded adequate model fit (as indicated by posterior predictive checking) (Muthén, 2010).

DSEM is a fusion of time series modeling, structural equation modeling, time-varying effects modeling, and multilevel modeling that combines aspects of each technique into a single framework (Asparouhov et al., 2018). Specifically, observed scores are decomposed into a temporally invariant, person-specific mean (μ; between-individual portion of the model), as well as an individual's deviation from their unique mean at a given time point (within-individual portion of the model). At the within-individual portion of the model, autoregressive effects are estimated by regressing within-person-centered scores at a given occasion ($score_t$) on the previous occasion's score ($score_{t-1}$) and/or additional prior scores (e.g., $score_{t-2}$, $score_{t-3}$, etc.). The omnibus effect of these autoregressive regression coefficients (ϕ) is modeled at the between-person level as a random slope (i.e., that varies between individuals). The ϕ parameter is often interpreted as the degree of carryover or inertia from one occasion to the next, as it captures the extent to which deviation at a given occasion predicts deviation at the next occasion(s). For example, a high ϕ parameter would indicate that if an individual's score at *t*-1 was above their average, it is also more likely to be above average at *t* (i.e., compared to if ϕ was lower).

The residual variance of the autoregressive effects (i.e., innovation variance) can also be allowed to differ across individuals such that a third random parameter is estimated at the between-person level, the random innovation variance ($\log[\sigma^2]$, computed as the log of the variance). The random innovation variance term simply represents the variability in a score at a given occasion that is not explained by the previous occasion's score (or occasions' depending on how the autoregressive effects are specified). As such, it can be considered to represent volatility or reactivity.

See Fig. 1 for the decomposition of DSEM model parameters. In the current study, we analyzed body temperature data collected in the morning and afternoon on six consecutive days. Due to normal diurnal fluctuations in body temperature (Harding et al., 2019; Heller et al., 2011; Refinetti and Menaker, 1992), it is likely that an individual's temperature at a given occasion is related to the temperature at the same time on the previous day (*t*-2), in addition to the previous measurement (*t*-1). Accordingly, we included separate autoregressive parameters for each pattern, henceforth referred to as Φ(1) for the relationship between a score and the previous score at *t*-1, and Φ(2) for the relationship between a score and the previous score at *t*-2 (i.e., at the same time the previous day). In addition to these autoregressive parameters, individuals' mean temperatures, and the random innovation variance, we also computed variables representing the peak temperature across the study period, as well as the day that peak occurred.

In the first iteration of the DSEM model, no between-level predictors were included. We used the results of this null model when exporting estimates of key parameters (specifically the mean estimate of the posterior distribution). In MPlus, a Bayesian framework is used to estimate DSEM models (Muthén, 2010), which employs a Markov Chain Monte Carlo algorithm with the option of a user-specified iteration number. Posterior parameter distributions are generated with means, medians, modes, and credibility intervals, as well as one-tailed *p* values. Per convention, we specified a minimum of 5,000 iterations and considered effects statistically significant only if the credibility intervals did not contain 0 (Asparouhov et al., 2018; Buysse et al., 1989; Muthén, 2010).

After estimating the null model, we included whether the participant became infected with the challenge virus as a between-level predictor of each parameter (see "Difference" column of Table 1 for results). We also examined whether these parameters differed by the type of challenge virus used (see Table S2 and Figure S1 for results by challenge virus). Upon exporting estimates of parameter values for each individual, we tested a series of regression models to examine relationships among temporal dynamics of body temperature in those infected with the challenge virus and objective/subjective symptoms, inflammation, and stress hormones. Separate models were tested for each construct due to missing data patterns attributable to differences in which variables were collected in each study of the CCP. Follow-up analyses controlled for the aforementioned covariates (see Table S3 for relationships between temperature and covariates; see Table S4 for results of secondary models controlling for covariates). The pattern of results was generally unchanged when controlling for covariates Table 2.

3. Results

Throughout the results section, *b* refers to unstandardized regression coefficients and *β* refers to standardized coefficients. CIs refer to credibility intervals for the effect generated by Bayesian estimation and can be interpreted in the same fashion as confidence intervals. Specifically, effects were considered significant only if the Cis did not contain 0. Mean temperatures are denoted by μ throughout the results section. Φ refers to omnibus autoregressive effects aggregated across time points; the regression of temperature scores at *t* on scores at *t*-1 is denoted Φ(1) and the regression of scores at *t* on scores at *t*-2 (same time on previous day) is denoted Φ(2). These autoregressive effects can be interpreted as the strength of relationships between changes to temperatures measured closely in time. The random innovation variance is represented by log (σ^2); this parameter refers to residual variance not explained by the

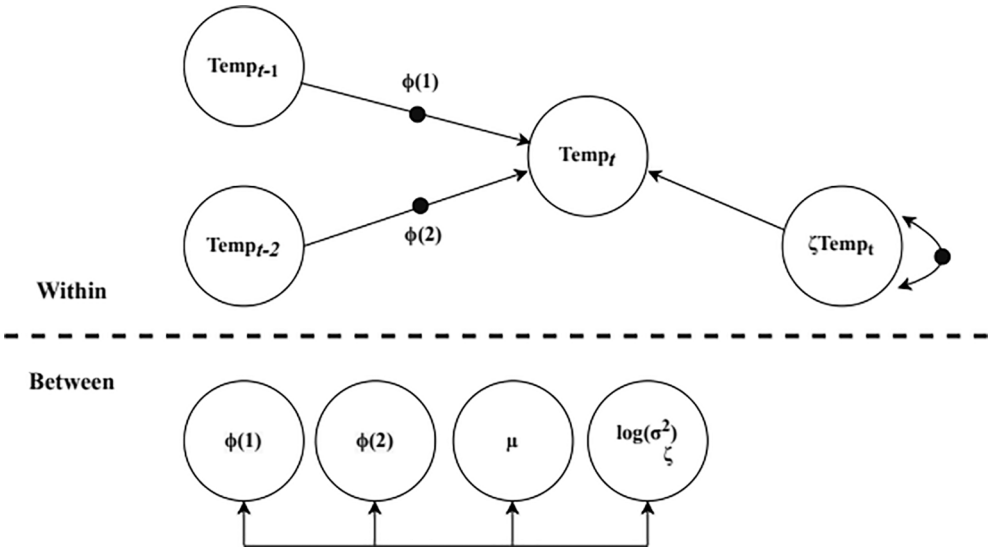

Fig. 1. Illustration of dynamic structural equation model decomposition. At level 1 (within-participant), temperature (*t*) is regressed on the previous temperature (*t*-1) and the measurement at the same time on the previous day (*t*-2). These parameters are modeled as random effects at level 2 (between-participants) as indicated by black circles; the residual variances after accounting for these effects are also modeled at level 2 as a random innovation term. This results in four key parameters: participants' mean temperature across quarantine (μ), the two autoregressive parameters (ϕ), and the random innovation variance log(σ^2).

Table 1
Impact of Infection on Body Temperature Dynamics.

	Not Infected(n = 302; 21.34%)				Infected(n = 1113; 78.66%)				Difference			
Parameter	**Estimate**	**Posterior *SD***	**Lower *CI***	**Upper *CI***	**Estimate**	**Posterior *SD***	**Lower *CI***	**Upper *CI***	**Estimate**	**Posterior *SD***	**Lower *CI***	**Upper *CI***
Mean (°F)	97.11	0.06	96.99	97.23	97.38	0.03	97.32	97.44	0.24*	0.06	0.11	0.36
Φ(1)	0.11	0.03	0.06	0.16	0.06	0.02	0.03	0.09	−0.06*	0.02	−0.10	−0.01
Φ(2)	0.49	0.03	0.44	0.54	0.44	0.02	0.41	0.47	−0.05*	0.03	−0.10	−0.003
log(σ^2)	−0.87	0.05	−0.97	−0.78	−0.90	0.02	−0.94	−0.85	−0.03	0.05	−0.13	0.07
Peak (°F)	98.13	0.05	98.03	98.23	98.38	0.03	98.32	98.43	0.24*	0.06	0.14	0.35
Day Peak	2.74	0.11	2.53	2.92	2.88	0.06	2.77	2.97	0.14	0.12	−0.08	0.41

autoregressive effects and can be interpreted as volatility or reactivity.

As is shown in Fig. 2, the two autoregressive parameters (Φ) each impact temperature stability, but the resulting pattern is highly dependent on the random innovation variance (log[σ^2]). For example, the blue line has a high Φ(2) parameter (regression of temperature on value measured at the same time on the previous day), and because log(σ^2) is low, there is a clear diurnal rhythm. With the gray line, the relative decrease in log(σ^2) and Φ(2), along with a small increase in Φ(1) (regression of temperature on previous measurement), yields a more consistent, flat pattern than the blue line. The yellow and orange lines each have higher log(σ^2), which is reflected in the more dramatic fluctuations over time. This is particularly evident in the pattern of the yellow line as the participant's body temperature elevates to the febrile range on Day 2 and then falls back down to a more stable baseline for the remainder of the study.

3.1. Impact of infection on body temperature dynamics

As shown in Table 1, body temperature tended to peak between Day 2 and Day 3 of quarantine, and this result did not differ based on whether or not the participant met the criteria for infection (b = 0.14, CIs = [-0.08, 0.41]). Overall, the viral challenge did not elicit an intense febrile response, which is typical for the common cold. Only 29.5% and 0.3% of participants who did not meet the criteria for infection exhibited any temperature above 98.6°F (37 °C) or 100.4°F (38 °C), respectively. On the other hand, 37.0% of those meeting the criteria for infection had a body temperature above 98.6°F (37 °C), and 0.8% had a temperature above 100.4°F (38 °C).

As is reported in Table 1 and displayed visually in Fig. 3, mean temperatures (μ) were slightly higher for those experiencing infection (97.38°F; 36.32 °C) compared to those who did not meet these criteria (97.11°F; 36.17 °C) (b = 0.24, CIs = [0.11, 0.36]). Similar results were found for peak temperatures (not infected: 98.13°F; 36.74 °C, infected: 98.38°F; 36.88 °C) (b = 0.24, CIs = [0.14, 0.35]). Results revealed that the autoregressive parameter estimates were much higher for the relationship between temperatures taken at the same time of day (Φ[2] relative to the prior measurement (Φ[1]), suggesting strong effects of diurnal rhythms. Both of these autoregressive parameters were higher for those not infected than those infected (Φ (1): b = -0.06, CIs = [-0.10, −0.01]; Φ (2): b = -0.05, CIs = [-0.10, −0.003]), indicating that infection was associated with less consistency across temperature measurements close together in time. There were no significant differences between these two groups in temperature volatility, which is reflected in the random innovation variance term (b = -0.03, CIs = [-0.13, 0.07]). In sum, in the context of infection, higher mean and peak temperatures were observed, but the extent to which one temperature value predicted the next was attenuated.

3.2. Relationships between body temperature dynamics and symptoms

Results of regression analyses are displayed in Table 3; significant effects as determined by credibility intervals are accompanied by an asterisk in the table. Results revealed that subjective symptoms did not appear to be related to any of the body temperature parameters (μ: β = 0.16, CIs = [-0.10, 0.33]; Φ[1]: β = 0.07, CIs = [−0.01, 0.16]; Φ[2]: β = 0.02, CIs = [-0.10, 0.13]; log(σ2): β = 0.14, CIs = [-0.06, 0.32]; peak temperature: β = -0.03, CIs = [−0.15, 0.08]). However, it is worth noting that the overwhelming majority of patients never reached febrile temperatures, and in general, few experienced intense symptoms. Accordingly, it is possible that synchrony between body temperature and symptoms would emerge in the context of more severe illness.

Higher baseline virus-specific antibody titers were associated with

Table 2
Results of Models Exploring Relationships between Temperature Dynamics, Features of Illness, and Stress Hormones.

	μ			Φ(1)			Φ(2)			$\log(\sigma^2)$			Peak Temperature			
Parameter	*β*	**LowCI**	**HighCI**	*β*	**LowCI**	**HighCI**	*β*	**LowCI**	**HighCI**	*β*	**LowCI**	**HighCI**	*β*	**LowCI**	**HighCI**	**PPP**
Objective andSubjective Symptoms																0.25
BaselineAntibodies	−0.06*	−0.12	−0.002	0.04	−0.02	0.10	0.03	−0.03	0.09	0.01	−0.05	0.07	−0.07*	−0.13	−0.01	
Post-ChallengeAntibodies	−0.09	−0.25	0.09	−0.01	−0.08	0.07	−0.03	−0.13	0.06	−0.18*	−0.34	−0.01	0.02	−0.09	0.13	
MucusProduction	0.14	−0.07	0.32	0.12*	0.04	0.21	−0.03	−0.14	0.08	0.10	−0.11	0.29	0.08	−0.03	0.19	
ViralShedding	0.13	−0.08	0.32	−0.06	−0.14	0.01	0.06	−0.05	0.14	0.14	−0.06	0.32	0.08	−0.03	0.19	
Subjective Symptom Score	0.16	−0.10	0.33	0.07	−0.01	0.16	0.02	−0.10	0.13	0.14	−0.06	0.32	−0.03	−0.15	0.08	
Nasal CytokineResponse																0.15
InflammationLatent Factor	−0.14*	−0.22	−0.05	0.13*	0.06	0.21	0.14*	0.06	0.22	0.05	−0.06	0.14	−0.16*	−0.23	−0.10	
StressHormones																0.33
SalivaryCortisol AUC	0.14*	0.04	0.25	−0.20*	−0.30	−0.09	−0.14*	−0.25	−0.03	−0.05	−0.16	0.07	0.15*	0.04	0.25	
Urinary CatecholamineOutput	−0.42*	−0.55	−0.29	0.24*	0.09	0.43	−0.06	−0.20	0.12	0.36*	0.22	0.494	−0.30*	−0.45	−0.17	

lower peak (β = -0.07, CIs = [-0.13, −0.01]) and average temperatures (μ: β = -0.06, CIs = [-0.12, −0.002]), but not other temperature parameters (Φ[1]: β = 0.04, CIs = [-0.02, 0.10]; Φ[2]: β = 0.03, CIs = [-0.03, 0.09]; log(σ2): β = 0.01, CIs = [-0.05, 0.07]). This may indicate that individuals' pre-existing humoral immunity attenuated the thermal response to infection, resulting in lower average temperatures (compared to those with lower baseline antibodies). For the most part, body temperature parameters were not related to post-challenge antibody titers (μ: β = -0.09, CIs = [-0.25, 0.09]; Φ[1]: β = -0.01, CIs = [-0.08, 0.07]; Φ[2]: β = -0.03, CIs = [-0.13, 0.06]; peak temperature: β = 0.02, CIs = [-0.09, 0.13]). However, lower random innovation variance was associated with higher post-challenge titers (log(σ2): β = -0.18, CIs = [-0.34, −0.01]). In other words, less temperature volatility during the study period predicted higher levels of challenge virus-specific antibodies after the study. This effect, however, became non-significant when controlling for covariates (see Table S4).

While no significant relationships between viral shedding and body temperature emerged (μ: β = 0.13, CIs = [-0.08, 0.32]; Φ[1]: β = -0.06, CIs = [-0.14, 0.01]; Φ[2]: β = 0.06, CIs = [-0.05, 0.14]; log(σ2): β = 0.14, CIs = [-0.06, 0.32]; peak temperature: β = 0.08, CIs = [-0.03, 0.19]), a higher Φ(1) parameter was associated with greater mucus production (β = 0.12, CIs = [0.04, 0.21]). This suggests that consistency in temperatures close in time was related to sustained production of mucus. However, it is unclear why this pattern of results emerged and mucus production was not related to other temperature parameters (μ: β = 0.14, CIs = [-0.07, 0.32]; Φ[2]: β = -0.03, CIs = [-0.14, 0.08]; log(σ2): β = 0.10, CIs = [-0.11, 0.29]; peak temperature: β = 0.08, CIs = [-0.03, 0.19]).

3.3. Relationships between body temperature dynamics and nasal cytokines

Results revealed moderate to strong factor loadings for the latent inflammation factor (IFN-α: β = 0.99, IL-1β: β = 0.90, TNF-α: β = 0.87, IL-8: β = 0.99, IL-6: β = 0.53; all CIs indicated statistical significance). As is shown in Table 3, higher levels of nasal cytokines were associated with lower peak (β = -0.16, CIs = [-0.23, −0.10]) and mean temperatures (β = -0.14, CIs = [-0.22, −0.05]) in subjects meeting the criteria for infection. Moreover, higher levels of nasal inflammation were also associated with stronger autoregressive effects (or temporal stability) (Φ[1]: β = 0.13, CIs = [0.06, 0.21]; Φ[2]: β = 0.14, CIs = [0.06, 0.22]), but not residual dynamic error (β = 0.05, CIs = [-0.06, 0.14]). In other words, as levels of inflammation increased, so did the strength of relationships between subsequent temperature measurements. Together, these results suggest that elevated nasal inflammation in the context of the common cold corresponds to lower, more consistent body temperatures across time.

3.4. Relationships between body temperature dynamics and stress hormones

Strong factor loadings were observed for the latent urinary catecholamine factor (epinephrine: β = 0.92, norepinephrine: β = 0.99, dopamine: β = 0.92; all CIs indicated statistical significance). Results revealed that baseline sympathetic nervous system and hypothalamic–pituitaryadrenal axis activity had differential impacts on temperature parameters. Specifically, as is shown in Table 3, higher levels of salivary cortisol over the course of the first day of quarantine were associated with higher mean (β = 0.14, CIs = [0.04, 0.25]) and peak temperatures (β = 0.15, CIs = [0.04, 0.25]), as well as weaker autoregressive effects (or temporal stability) (Φ[1]: β = -0.20, CIs = [-0.30, −0.09]; Φ[2]: β = -0.14, CIs = [-0.25, −0.03]), but not residual dynamic error (β = -0.05, CIs = [-0.16, 0.07]). On the contrary, greater urinary catecholamine output was related to lower mean (β = -0.42, CIs = [-0.55, −0.29]) and peak temperatures (β = -0.30, CIs = [-0.45, −0.17]), higher Φ(1) (β = 0.24, CIs = [0.09, 0.43]), and greater residual dynamic

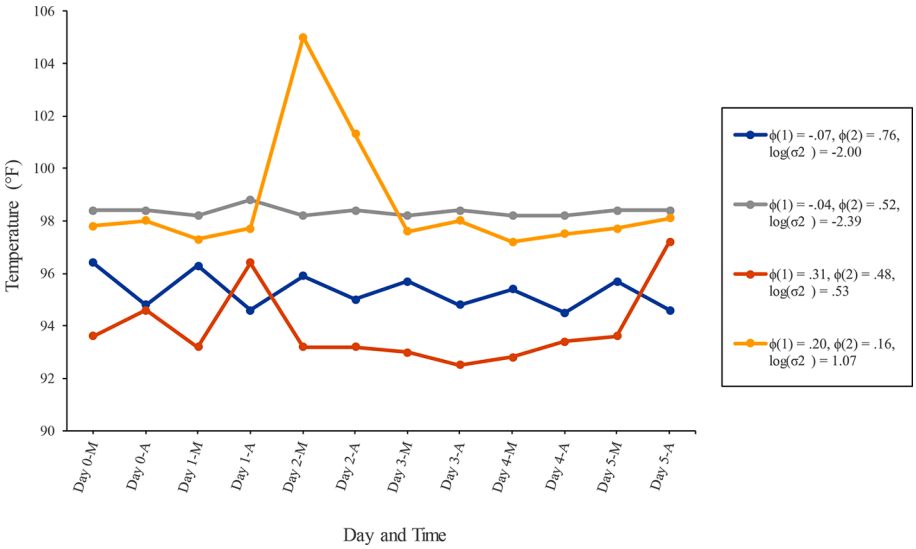

Fig. 2. Real participant data demonstrating how changes in temperature parameters are reflected in temporal dynamics across six days of quarantine. ϕ refers to the autoregressive parameters of current temperature on the previous temperature (Φ[1] and the temperature at the same time the previous day (Φ[2], log(σ^2) refers to the random innovation term reflecting residual variance unaccounted for by the autoregressive parameters. F = Fahrenheit, M = morning, A = afternoon.

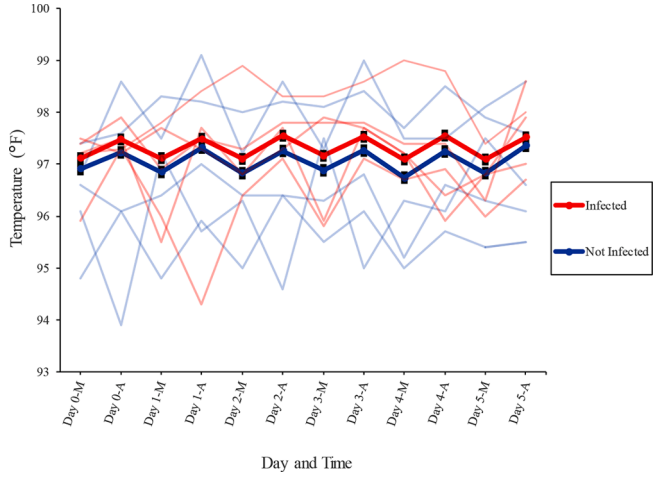

Fig. 3. Visual depiction of differences in temporal dynamics of body temperature between those who did (red lines) and did not (blue lines) meet the criteria for infection across six days of quarantine. Bold line trajectories are based on group means. Faint lines reflect actual data from a random subset of five participants in each condition. F = Fahrenheit, M = morning, A = afternoon. (For interpretation of the references to colour in this figure legend, the reader is referred to the web version of this article.)

error (β = 0.36, CIs = [0.22, 0.49]). In other words, higher levels of cortisol predicted higher temperatures with low consistency from one measurement to the next. On the other hand, higher levels of catecholamines predicted lower temperatures, with strong relationships between successive measurements and a large amount of residual variance unaccounted for by these relationships. Together, these findings reveal complex interactions between stress hormones and body temperature during the common cold that may reflect intricate processes of energy regulation and thermogenesis in this context. We discuss possible explanations for these results in the Discussion.

Follow-up models involved repeating the analyses while controlling for a variety of demographic and health variables (see Method section for full list). Overall, the pattern of results was largely unchanged when controlling for these covariates. Relationships between temperature dynamics and covariates are displayed in Table S3; see Table S4 for results of follow-up models controlling for covariates.

4. Discussion

The current research utilized a DSEM framework to explore links between temporal dynamics of body temperature change following an experimental respiratory virus challenge, inflammation, and other features of infection. Further, we examined how these temperature dynamics, including mean temperature, peak temperature, autoregressive parameters, and residual variance, were influenced by individual differences in levels of stress hormones (i.e., salivary cortisol and urinary catecholamine output). Results revealed that in addition to impacting absolute temperature values, infection also exerted effects on the strength of intra- and inter-day relationships. Specifically, those meeting the criteria for infection (compared to those who did not) exhibited higher mean and peak temperatures with less consistency between subsequent measurements and reduced diurnal regularity. Without data bearing directly on the mechanisms underlying these findings, caution should be exercised when interpreting them. However, the temporal instability that accompanies rising temperatures might reflect energy constraints that occur during infection. The innate immune response to acute infection bears tremendous energetic costs (Barr et al., 1922; Elia, 1992; Muehlenbein et al., 2010), which may limit the body's ability to efficiently regulate temperature in this context.

The current project also yielded interesting, if not unexpected, findings regarding the relationship among temperature dynamics, inflammation, and stress hormones. First, higher levels of nasal proinflammatory cytokines were associated with lower, more consistent temperatures during the study. At face value, this is surprising given the pyrogenic nature of these cytokines (BLATTEIS and SEHIC, 1998; Coiffard et al., 2021; Saper and Breder, 1992;93:419–28). However, it is important to keep in mind that cytokine levels in nasal wash samples may not necessarily reflect systemic levels (Hayden et al., 1998). Moreover, it is possible that higher body temperature, within a healthy range, enhances the efficiency of the immune response, resulting in less inflammation and tissue damage in the upper respiratory tract (Evans et al., 2015; Schieber et al., 2016; Small et al., 1986).

Also of interest was the contrasting effects that levels of salivary cortisol and urinary catecholamines had on temperature parameters. Specifically, higher cortisol levels on the first day of quarantine were related to higher, less temporally stable temperatures. This finding is

consistent with the hypothesis that elevated glucocorticoid signaling at baseline increases the energetic resources available for heat generation (Kuo et al., 2016). However, less clear is why higher cortisol would be associated with less temperature consistency. One possibility is that this pattern is produced by a tug-of-war between catabolic and immunoregulatory features of glucocorticoids (Riccardi et al., 2002; Kuo et al., 2016). That is, high levels of cortisol may increase the energy available for thermoregulation, but also exert suppressive effects on immune cells that release pyrogenic cytokines. A perhaps more likely possibility is that, in general, high temperatures are just usually less stable given the metabolic costs of heat generation (Muehlenbein et al., 2010). This latter explanation is supported by the finding that those infected tended to have higher, less consistent temperatures than those not infected by challenge viruses.

On the other hand, higher catecholamine levels predicted lower temperatures with strong diurnal effects, but substantial residual variance (i.e., volatility or reactivity). This finding is unexpected given the effects of catecholamines on vasomotor responses that prevent heat dissipation (BLATTEIS and SEHIC, 1998; Coiffard et al., 2021; Saper and Breder, 1992;93:419–28). However, it is worth highlighting that the 24-hr urine collection took place on the first day of quarantine (with a second measurement pre-quarantine for some participants). Accordingly, high values of catecholamines in this study represent higher baseline levels of these neurotransmitters in the periphery, as opposed to an infection-induced increase. While this is purely speculative, elevated catecholamines in the periphery could result in resistance to these neurotransmitters at target tissues. Other research has shown this can occur in adipose tissue, particularly in the context of inflammation (Mowers et al., 2013). Non-human animal research examining the impact of stress pre-exposure to subsequent generation of fever may lend further insights these findings (Hayden et al., 1998; Mowers et al., 2013). Specifically, studies find that restraint stress pre-exposure attenuates the febrile response to antigens like lipopolysaccharide. In the current research, higher baseline catecholamine levels may indicate greater stress which, in turn, could impair the thermic response to infection.

As with any study, the current research has limitations that should be considered. First, temperature was only measured twice each day. This represents a major limitation, as it adds uncertainty to the estimation of autoregressive parameters, diurnal effects, and mean temperatures. Moreover, measurements closer in time would likely yield much stronger autoregressive effects and minimize unexplained variance. Future studies would benefit from continuous temperature monitoring over the course of one or several days, which would also help ease sample size requirements for DSEM (Hecht and Zitzmann, 2021). Further, given the experimental design of the research, only viruses that cause mild illness could be used for ethical reasons. Additional research is needed to investigate whether the pattern of results found here generalize to those experiencing more severe illness, perhaps even in the context of COVID-19. Next, due to the timing of data collection and patterns of missing data, inflammation and stress hormones were modeled using AUC values. Accordingly, we could not compare the temporal dynamics of these variables to those of body temperature across the same period. Doing so with vector autoregressive or other multivariate time series models may offer key insights into the mechanisms underlying the effects observed here.

Also important to consider is that there were several differences between CCP studies including, but not limited to, methods of temperature sampling and the challenge viruses used. While we controlled for study number and challenge virus in all analyses, it is impossible to completely account for between-study variability statistically. Accordingly, these results should be interpreted with due caution and considered in light of the differences between study methods reported in the Method section and differences between viruses shown in Table S2. The parameter estimates most likely to be affected by methodological heterogeneity are mean and peak temperatures, as oral and aural temperatures fluctuate between slightly different ranges. On the other hand, autoregressive and residual variance parameters should be less sensitive to temperature scale given that they are based on within-individual score regressions. However, even if the estimates of mean and peak temperatures are biased by methodological differences between studies, this does not necessarily skew the results of the primary statistical tests. For example, the significance of relationships between inflammation and mean temperatures does not depend on variable absolute values, but rather on how relative changes to one variable impact relative changes to the other.

As a final note, the current project demonstrates the utility of DSEM for studying time-dependent changes in biological variables. It is important to carefully consider the sample size and occasion number requirements before attempting to fit data to a DSEM model (or any time series model; (Hecht and Zitzmann, 2021). Nonetheless, when these requirements are met, DSEM and other dynamic models (e.g., slope entropy) (Cuesta-Frau et al.,) allow for estimating a comprehensive set of parameters that may better capture the reality of biological complexity and individual differences than some commonly used longitudinal models (Harrison et al., 2018; Pinheiro and Bates, 2000; Preacher et al., 2008). For example, in Fig. 3, the bold lines generated from time-specific group means clearly illustrate the differences between the two groups (i.e., not infected vs. infected) in average temperature. However, the more transparent lines, which represent temperatures from a random subset of five participants who met the criteria for infection and five participants who did not, show that the patterns of group means are not generally consistent with actual participants' data. Depending on one's research question, this may be important to consider before assuming that participants' means converge on a common trajectory, as is often done in mixed-effects and growth curve modeling (Harrison et al., 2018; Pinheiro and Bates, 2000; Preacher et al., 2008), or even AUC computation (Lopez-Duran et al., 2014). These approaches are very useful in many circumstances, and some are even employed in the current research. Moreover, many can be modified to obtain additional parameters (Lopez-Duran et al., 2014). However, as shown in Fig. 3, a large amount of information can be lost when individual variation is solely examined in the form of random intercepts and slopes, and error is treated as a nuisance rather than a possibly biologically meaningful parameter.

Declaration of Competing Interest

The authors declare that they have no known competing financial interests or personal relationships that could have appeared to influence the work reported in this paper.

Acknowledgments

The data were collected by the Laboratory for the Study of Stress, Immunity, and Disease at Carnegie Mellon University under the directorship of Sheldon Cohen, Ph.D.; and were accessed via the Common Cold Project website (www.commoncoldproject.com).

Funding

The grant that supports the Common Cold Project is NCCIH AT006694. The grants that provided primary funding for the research study or studies whose data are used were: NIMH MH50429, NHLBI HL65111, HL65112, and NIAID R01 AI066367. The grants that supported clinical and regulatory assistance to the studies were: NIH 5 M01 RR00056, NIH UL1 RR024153, and UL1 TR0005.

Appendix A. Supplementary data

Supplementary data to this article can be found online at https://doi.org/10.1016/j.bbi.2021.10.001.

References

Al-Nakib, W., Tyrell, D.A.J., 1988. Picornaviridae: Rhinoviruses—Common Cold Viruses. In: Lennette, E.H., Halonen, P., Murphy, F.A. (Eds.), Laboratory Diagnosis of Infectious Diseases Principles and Practice: VOLUME II Viral, Rickettsial, and Chlamydial Diseases. Springer-Verlag, New York.

Al-Nakib, W., Dearden, C.J., Tyrrell, D.A.J., 1989. Evaluation of a new enzyme-linked immunosorbent assay (ELISA) in the diagnosis of rhinovirus infection. J. Med. Virol. 29 (4), 268–272.

Angilletta, M.J., Cooper, B.S., Schuler, M.S., et al., 2010. The evolution of thermal physiology in endotherms. Front. Biosci. Elite Ed. 2, 861–881.

Asparouhov, T., Hamaker, E.L., Muthén, B., 2018. Dynamic Structural Equation Models. Struct. Equ. Model Multidiscip. J. 25 (3), 359–388.

Barclay, W.S., Al-Nakib, W., 1987. An ELISA for the detection of rhinovirus specific antibody in serum and nasal secretion. J. Virol. Methods 15 (1), 53–64.

Barr, D., Russell, M., Cecil, L., et al., 1922. Clinical calorimetry XXXII: temperature regulation after the intravenous injections of protease and typhoid vaccine. Arch. Int. Med. 608–634.

Biddle, C., 2006. The neurobiology of the human febrile response. AANA J 74, 145–150.

Blatteis CM, Sehic E. Cytokines and Fever. Ann. N Y Acad. Sci. 1998;840:608–18.

Buysse, D.J., Reynolds, C.F., Monk, T.H., Berman, S.R., Kupfer, D.J., 1989. The Pittsburgh Sleep Quality Index: a new instrument for psychiatric practice and research. Psychiatry Res. 28 (2), 193–213.

Cohen, S., Alper, C.M., Doyle, W.J., Treanor, J.J., Turner, R.B., 2006. Positive emotional style predicts resistance to illness after experimental exposure to rhinovirus or influenza a virus. Psychosom. Med. 68 (6), 809–815.

Cohen, S., Janicki-Deverts, D., Doyle, W.J., Miller, G.E., Frank, E., Rabin, B.S., Turner, R. B., 2012. Chronic stress, glucocorticoid receptor resistance, inflammation, and disease risk. Proc. Natl. Acad. Sci. U.S.A. 109 (16), 5995–5999.

Coiffard, B., Diallo, A.B., Mezouar, S., Leone, M., Mege, J.-L., 2021. A Tangled Threesome: Circadian Rhythm, Body Temperature Variations, and the Immune System. Biology 10 (1), 65. https://doi.org/10.3390/biology10010065.

Cuesta-Frau D, Dakappa PH, Mahabala C et al. Fever Time Series Analysis Using Slope Entropy. Application to Early Unobtrusive Differential Diagnosis. Entropy 2020;22: 1034.

Doyle, W., Casselbrant, M., Li-Korotky, H.-S., Cullen Doyle, A., Lo, C.-Y., Turner, R., Cohen, S., 2010. The Interleukin 6–174 C/C Genotype Predicts Greater Rhinovirus Illness. J. Infect. Dis. 201 (2), 199–206.

Dressendörfer, R.A., Kirschbaum, C., Rohde, W., Stahl, F., Strasburger, C.J., 1992. Synthesis of a cortisol-biotin conjugate and evaluation as a tracer in an immunoassay for salivary cortisol measurement. J. Steroid Biochem. Mol. Biol. 43 (7), 683–692.

Drewry, A.M., Fuller, B.M., Bailey, T.C., Hotchkiss, R.S., 2013. Body temperature patterns as a predictor of hospital-acquired sepsis in afebrile adult intensive care unit patients: a case-control study. Crit. Care Lond. Engl. 17 (5), R200. https://doi.org/10.1186/cc12894.

Elia, M., 1992. Energy expenditure to metabolic rate. *Energy Metabolism: Tissue Determinants and Cellular Corollaries*. Raven Pr, New York, pp. 19–49.

Evans, S.S., Repasky, E.A., Fisher, D.T., 2015. Fever and the thermal regulation of immunity: the immune system feels the heat. Nat. Rev. Immunol. 15 (6), 335–349.

Gagge A, Gonzalez R. Mechanisms of Heat Exchange: Biophysics and Physiology. 2011: 45–84.

Geneva II, Cuzzo B, Fazili T et al. Normal Body Temperature: A Systematic Review. Open Forum Infect Dis 2019;6:ofz032.

Geneva, I.I., Javaid, W., 2020. Disruption of the Body Temperature Circadian Rhythm in Hospitalized Patients. Open Forum Infect. Dis. 7, S631.

GENSINI, G., CONTI, A., 2004. The evolution of the concept of "fever" in the history of medicine: from pathological picture per se to clinical epiphenomenon (and vice versa). J. Infect. 49 (2), 85–87.

Gwaltney, J.M.J., Colonno, R.J., Hamparian, V.V., et al., 1989. Rhinovirus. In: Schmidt, N.J., Emmons, R.W. (Eds.), Diagnostic Procedures for Viral, Rickettsial and Chlamydial Infections, 6th edition. Amer Public Health Assn, Washington, DC, pp. 579–614.

Harding, C., Pompei, F., Bordonaro, S.F., McGillicuddy, D.C., Burmistrov, D., Sanchez, L. D., 2019. The daily, weekly, and seasonal cycles of body temperature analyzed at large scale. Chronobiol. Int. 36 (12), 1646–1657.

Harrison XA, Donaldson L, Correa-Cano ME et al. A brief introduction to mixed effects modelling and multi-model inference in ecology. PeerJ. 2018;6:e4794.

Hayden, F.G., Fritz, R., Lobo, M.C., Alvord, W., Strober, W., Straus, S.E., 1998. Local and systemic cytokine responses during experimental human influenza A virus infection. Relation to symptom formation and host defense. J. Clin. Invest. 101 (3), 643–649.

Hecht, M., Zitzmann, S., 2021. Sample Size Recommendations for Continuous-Time Models: Compensating Shorter Time Series with Larger Numbers of Persons and Vice Versa. Struct. Equ. Model Multidiscip. J. 28 (2), 229–236.

Heller, H.C., Edgar, D.M., Grahn, D.A., et al., 2011. Sleep, Thermoregulation, and Circadian Rhythms. Compr. Physiol. 1361–1374.

Huitron-Resendiz, S., Marcondes, M.C.G., Flynn, C.T., Lanigan, C.M.S., Fox, H.S., 2007. Effects of simian immunodeficiency virus on the circadian rhythms of body temperature and gross locomotor activity. Proc. Natl. Acad. Sci. 104 (38), 15138–15143.

Jackson, G.G., Dowling, H.F., Spiesman, I.G., et al., 1958. Transmission of the common cold to volunteers under controlled conditions. I. The common cold as a clinical entity. AMA Arch. Intern. Med. 101, 267–278.

Jessen, C., 2012. Temperature Regulation in Humans and Other Mammals. Springer Science & Business Media.

Kuo T, McQueen A, Chen T-C et al. Regulation of Glucose Homeostasis by Glucocorticoids. Glucocorticoid signaling, 99-126. Laboratory for the Study of Stress, Immunity, and Disease. (2016). Common Cold Project. Retrieved from http://www.commoncoldproject.com. 2015.

Lennette NJ, Schmidt EH. 1979. Diagnostic Procedures for Viral, Rickettsial and Chlamydial Infections. 5th Revised edition. Washington D.C: American Public Health Association Publications, Washington, DC, U.S.A.

Lopez-Duran, N.L., Mayer, S.E., Abelson, J.L., 2014. Modeling neuroendocrine stress reactivity in salivary cortisol: adjusting for peak latency variability. Stress Amst. Neth. 17 (4), 285–295.

McQuillin, J., Gardner, P.S., 1968. Rapid diagnosis of respiratory syncytial virus infection by immunofluorescent antibody techniques. Br. Med. J. 1 (5592), 602–605.

Mills, P.J., Ziegler, M.G., Rehman, J., et al., 1998. Catecholamines, catecholamine receptors, cell adhesion molecules, and acute stressor-related changes in cellular immunity. Adv. Pharmacol. San Diego Calif 42, 587–590.

Mowers J, Uhm M, Reilly SM et al. Inflammation produces catecholamine resistance in obesity via activation of PDE3B by the protein kinases IKKε and TBK1. Glass C (ed.). eLife 2013;2:e01119.

Muehlenbein, M.P., Hirschtick, J.L., Bonner, J.Z., Swartz, A.M., 2010. Toward quantifying the usage costs of human immunity: Altered metabolic rates and hormone levels during acute immune activation in men. Am. J. Hum. Biol. Off. J. Hum. Biol. Counc. 22 (4), 546–556.

Muthén, B.O., 2002. Beyond SEM: General latent variable modeling. Behaviormetrika 29 (1), 81–117.

Muthén B. 2010. Bayesian Analysis In Mplus: A Brief Introduction.

Pinheiro, J.C., Bates, D.M. (Eds.), 2000. Linear Mixed-Effects Models: Basic Concepts and Examples. *Mixed-Effects Models in S and S-PLUS*. Springer, New York, NY, pp. 3–56.

Preacher, D.K.J., Wichman, A.L., MacCallum, R.C., et al., 2008. Latent Growth Curve Modeling, 1st edition. SAGE Publications Inc, Los Angeles.

Ramsay, D.S., Woods, S.C., 2014. Clarifying the roles of homeostasis and allostasis in physiological regulation. Psychol. Rev. 121 (2), 225–247.

Ravanelli, N., Bongers, C.C.W.G., Jay, O., 2019. The Biophysics of Human Heat Exchange. In: Périard, J.D., Racinais, S. (Eds.), Heat Stress in Sport and Exercise: Thermophysiology of Health and Performance. Springer International Publishing, Cham, pp. 29–43.

Refinetti, R., Menaker, M., 1992. The circadian rhythm of body temperature. Physiol. Behav. 51 (3), 613–637.

Rezende, E.L., Bacigalupe, L.D., 2015. Thermoregulation in endotherms: physiological principles and ecological consequences. J. Comp. Physiol. [B] 185 (7), 709–727.

Riccardi, C., Bruscoli, S., Migliorati, G., 2002. Molecular mechanisms of immunomodulatory activity of glucocorticoids. Pharmacol. Res. 45 (5), 361–368.

Saper CB, Breder CD. Endogenous pyrogens in the CNS: role in the febrile response. Prog. Brain Res. 1992;93:419–28; discussion 428-429.

Schieber, A.M.P., Ayres, J.S., Napier, B., 2016. Thermoregulation as a disease tolerance defense strategy. Pathog. Dis. 74 (9), ftw106. https://doi.org/10.1093/femspd/ftw106.

Small, P.M., Täuber, M.G., Hackbarth, C.J., Sande, M.A., 1986. Influence of body temperature on bacterial growth rates in experimental pneumococcal meningitis in rabbits. Infect. Immun. 52 (2), 484–487.

Szelenyi, J., Vizi, E.S., 2007. The catecholamine cytokine balance: interaction between the brain and the immune system. Ann. N. Y. Acad. Sci. 1113 (1), 311–324.

Tobita, K., Sugiura, A., Enomoto, C., Furuyama, M., 1975. Plaque assay and primary isolation of influenza A viruses in an established line of canine kidney cells (MDCK) in the presence of trypsin. Med. Microbiol. Immunol. (Berl) 162 (1), 9–14.

Verburg-van Kemenade, B.M.L., Cohen, N., Chadzinska, M., 2017. Neuroendocrine-immune interaction: Evolutionarily conserved mechanisms that maintain allostasis in an ever-changing environment. Dev. Comp. Immunol. 66, 2–23.

Zhuang, X., Rambhatla, S.B., Lai, A.G., McKeating, J.A., 2017. Interplay between circadian clock and viral infection. J. Mol. Med. Berl. Ger. 95 (12), 1283–1289.

Ziegler, M.G., 2012. Psychological stress and the autonomic nervous system. In: Robertson, D.W., Biaggioni, I., Burnstock, G. (Eds.), Primer on the Autonomic Nervous System, 3rd ed. Elsevier Inc., pp. 291–293